HYDROLOGICAL PROCESSES
Hydrol. Process. **25**, 3347–3355 (2011)
Published online 15 June 2011 in Wiley Online Library
(wileyonlinelibrary.com) DOI: 10.1002/hyp.8170

A preliminary investigation of the influence of basal and surface topography on supraglacial lake distribution near Jakobshavn Isbrae, western Greenland

D. J. Lampkin[1,2]* and J. VanderBerg[1]

[1] *Department of Geography, College of Earth and Mineral Sciences, Pennsylvania State University, University Park, PA 16802, USA*
[2] *Department of Geoscience, College of Earth and Mineral Sciences, Pennsylvania State University, University Park, PA 16802, USA*

Abstract:

The spatial distribution of supraglacial lakes has been hypothesized to be dominantly controlled by the component of surface roughness influenced by basal topography. Basal topography and surface roughness profiles within the Jakobshavn Isbrae drainage basin in western Greenland, acquired from an ice-penetrating radar echo sounder, were analysed through fourier and wavelet decompositions. Spectral analyses of basal-to-surface transfer under a range of ice thickness were compared with spatial distribution of lakes mapped from high-resolution Landsat imagery. Fourier analysis identifies dominant signals in both the basal and surface profiles to be ranging between wavelengths of 1·25–12·5 km. The strongest peaks of transfer of basal signals to the surface were identified at wavelengths ∼11 ∼5 km. Wavelet analysis identifies these peaks with thicker (1200–1400 m) and thinner (500–700 m) ice respectively and also identifies surface frequencies not present in the basal signal indicating some influence from other factors. Spatial autocorrelation analysis of supraglacial lake distribution indentifies high correlations at 1·9, 5·6, 11, 24, and 30 km lags. Lags at 5·6 and 11 km correspond to dominant frequencies present in the basal and surface profiles over thinner and thicker ice respectively. These ∼5 and ∼11 km frequency components present in the basal topography, surface roughness, and lake distribution are within the theoretical transfer window of basal-to-surface transfer as a function of ice thickness. The transect analysed in this study does not contain wavelengths in the surface structure that are less than the ice thickness, even though there are relatively higher frequencies present in the surface profile between 0 and 15 km that have less power in the basal profile. Copyright © 2011 John Wiley & Sons, Ltd.

KEY WORDS supraglacial lakes; basal topography; Greenland ice sheet; surface melt

Received 22 July 2010; Accepted 9 May 2011

INTRODUCTION

The changing mass of the Greenland (GIS) and Antarctic ice sheets represents the largest unknown on predictions of global sea-level rise over the coming decades (Dowdeswell, 2006; IPCC, 2007). Recent estimates from GRACE (Gravity Recovery and Climate Experiment) indicate that GIS mass loss has accelerated from 137 Gt/yr measured over 2002–2003, to 286 Gt/yr measured over 2007–2009 (Velicogna, 2009). The GIS contribution to sea level more than doubled in the past decade, increasing from $0{\cdot}23 \pm 0{\cdot}08$ mm/yr in 1996, to $0{\cdot}57 \pm 0{\cdot}10$ mm/yr in 2005. Approximately half this mass loss is due to changes in the dynamics of a few large outlet glaciers (Rignot and Kanagaratnam, 2006; Stearns and Hamilton, 2007; Joughin *et al*., 2008; Van den Broeke *et al*., 2009). Jakobshavn Isbræ has perhaps undergone the most severe acceleration and thinning over the past decade (Joughin *et al*., 2004; Thomas *et al*., 2009). While the thinning and retreat of the ice tongue and the corresponding back force reduction is the dominant driving force of these changes (Luckman *et al*., 2006; Howat *et al*., 2008; Joughin *et al*., 2008; Thomas *et al*., 2009; Joughin *et al*., 2010), basal lubrication due to infiltration of surface meltwater is known to be a secondary but important factor. Coincident with the changes in flow dynamics on Jakobshavn is an increase in surface melt along the margins of GIS, resulting in enhanced meltwater infiltration to the ice sheet bed (Zwally *et al*., 2002). Meltwater infiltration to the base of the ice sheet is believed to have a significant impact on ice sheet flow behaviour (Zwally *et al*., 2002; Parizek and Alley, 2004; Shepard *et al*., 2009; Bartholomew *et al*., 2010). Meltwater runoff collects in surface depressions, forming numerous lakes that span several square kilometers and drain rapidly through a network of englacial channels (Weertman, 1973; Van der Veen, 1998; and Alley *et al*., 2005b). Recent studies have explained the transport of surface meltwater to the bed from lakes through the hydrofracture mechanism (Thomsen *et al*., 1988; Boon and Sharp, 2003; Alley *et al*., 2005a; Fountain *et al*., 2005; van der Veen, 2007; Das *et al*., 2008). Supraglacial lakes are a key component of the subglacial hydrologic system, therefore, improving our understanding of this system will

* Correspondence to: D. J. Lampkin, 313 Walker Building, University Park PA 16802, USA. E-mail: djl22@psu.edu

improve our ability to predict changes in ice sheet mass balance and contribution to sea level in response to future warming.

BACKGROUND

The ablation zone of the Greenland ice sheet is characterized by the presence of supraglacial lakes that form during the summer melt season. Lakes can span up to several square kilometers, with an increase in maximum extent from ~1450 m in 1991 to ~1600 m in 2007 (Echelmeyer *et al*., 1991; Luthje *et al*., 2006; Box and Ski, 2007; McMillan *et al*., 2007; Sundal *et al*., 2009). Several studies have speculated that the primary control of supraglacial lake distribution is the bedrock topography (Box and Ski, 2007; Das *et al*, 2008) given larger lakes tend to occur in the same location from season to season (Thomsen *et al*., 1988; Echelmeyer *et al*., 1991; Jezek *et al*., 1993). There is a need to better understand the relationship between surface (S) and basal (B) topographic roughness spectra. There have been several investigations examining basal-to-surface roughness transfer functions (Nye, 1959; Budd, 1970; Hutter *et al*., 1981; Whillans and Johnsen, 1983; Gudmudsson, 2003), mathematically expressed as $S(\lambda) = T(\lambda)B(\lambda)$, where transfer of basal spectral components (B) to surface spectral components (S) are controlled by the transfer function (T) (Budd, 1968, 1969). The functional form of $T(\lambda)$ can be strongly dependent on ice thickness (h). Budd and Carter (1971) established transfer functions with peak basal-to-surface transfer occurring at $\lambda \approx 3h$. Gudmundsson (2003) expands constraints on optimal transfer to $3h < B < 8h$ and explains that this range is a function of the regional surface slope and the relative influence of the mean rate of sliding at the base to the rate of internal deformation (basal slip ratio) integrated over h by influencing the horizontal transmission of stress gradients. At small to moderate slip ratios, the impact of local basal perturbations are limited, but at relatively larger slip ratios basal-to-surface amplitude increase (Gudmundsson, 2003). Therefore, basal roughness components corresponding to wavelengths between three and eight times the ice thickness are allowed to transfer to the surface topographic structure, whereas wavelengths outside this window are attenuated (Figure 2).

The transfer of basal roughness into ice sheet surface morphology has been theoretically established, but how basal structure influences the distribution of supraglacial lakes is still unresolved. Understanding the controls on supraglacial lake distribution and the mechanisms that facilitate the transport of surface melt and infiltration can provide critical insights into the evolution of GIS ablation zone. This study presents preliminary results from a comparison of the frequency decomposition of retrieved surface and basal topography and their relationship to supraglacial lake distributions over a limited transect spanning the ablation zone near Jakobshavn Isbrae. This work will provide initial insights into relationships between basal topography and those surface roughness components responsible for influencing the spatial distribution of supraglacial lakes.

STUDY AREA

This study examines how basal topographic variability transfers into surface roughness and the impact on the distribution of supraglacial lakes within the Jakobshavn Isbræ drainage basin region of Western Greenland (Figure 1). Jakobshavn is a large outlet glacier that drains ~7% of the Greenland ice sheet (Echelmeyer *et al*., 1991; Luckman and Murray, 2005). The highly dynamic Jakobshavn outlet glacier has experienced a rapid retreat over the last 15 years, coincident with rapid acceleration (Joughin *et al*., 2004). Additionally, the ablation zone within the Jakobshavn drainage basin is dominated by supraglacial lakes that fill and drain as the melt season evolves. The analysis in this investigation will focus on a 65 km transect, approximately 40 km south of the main trunk of Jakobshavn ice Stream, over ice thicknesses ranging from ~200 m to ~1400 m. The transect of interest spans a range in elevation from approximately 500–1300 m oriented parallel to the dominant ice flow direction and approximately parallel to the mass balance gradient. Ice in this immediate area exhibited a mean velocity of ~200 ma^{-1} in 2006, marking a slight deceleration since 2000 (Joughin *et al*., 2010).

DATA

This study uses surface elevation data derived from a digital elevation model (DEM), basal topography from the combination of airborne laser altimeter and ice penetrating radar, and a regional inventory of supraglacial lakes delineated from visible satellite imagery during the 2007 ablation season. Additionally, surface velocity grids derived from synthetic aperture radar (SAR) are used in this analysis.

Surface and basal elevation data

Surface elevations (Figure 3c) were extracted from a DEM constructed from visible stereo images acquired by the High Resolution Stereoscopy (HRS) sensor onboard the SPOT-5 satellite. The SPOT DEM has a 40 m horizontal spatial resolution and is referenced to the World Geodetic System (WGS) 1984 datum (http://polardali.spotimage.fr:8092/IPY/dalisearch.aspx).

Basal topography (H_b) (Figure 3d) was estimated based on measured surface elevation and ice thickness given by the following:

$$H_b = H_s - h \tag{1}$$

where H_s is surface elevation and h is ice thickness. Ice thickness data were acquired from the Center for

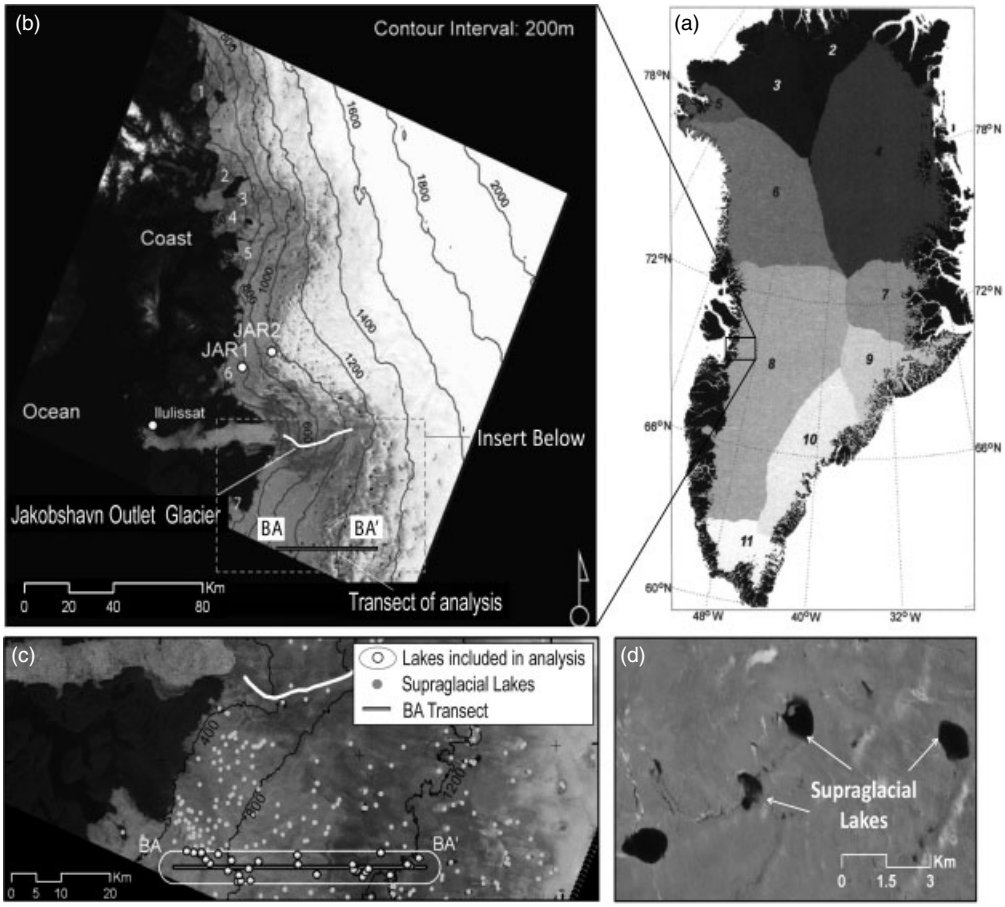

Figure 1. Study region: a) The study region boundaries are highlighted in the regional map depicting the relative location of Jakobshavn drainage basin located in western Greenland with delineated drainage basins (Hardy *et al*., 2000). b) The graph depicts the study region which is a large proportion of the ablation zone within the Jakobshavn drainage basin. The transect under analysis (BA to BA') is oriented longitudinally (parallel to the dominant ice flow direction) and is 65 km long, approximately 40 km south of the main trunk of Jakobshavn Isbrae. Elevation contours (200 m intervals) are superimposed over a 2007 grey-scale panchromatic Landsat-7 EMT+ image. c) This localized map of the transect displays the distribution of supraglacial lakes in this area. The map also identifies lakes selected for analysis along transect BA and shows distribution across elevation. d) A zoomed-in example of supraglacial lakes near thetransect of analysis from the Landsat imagery

Remote Sensing of Ice Sheets (CReSIS) Multichannel Coherent Radar Depth Sounder (MCoRDS) (Plummer *et al*., 2008; https://www.cresis.ku.edu/data/greenland). The MCoRDS instrument is aircraft mounted and produces a pulse of electromagnetic frequency at 140 MHz and measures the time of return of the signal off both the ice surface and bedrock below the ice. The difference in travel time is converted into distances and allows for a calculation of ice thickness. Subtracting the ice thickness from the surface topography produces a basal topographic profile that is referenced to the WGS84. This CReSIS data is collected along transects, spatially sampled at 15 m intervals.

Supraglacial lake inventory

Supraglacial lakes (Figure 1c) were delineated from high-resolution, cloud-free, Landsat-7, Enhanced Thematic Mapper Plus (ETM+) imagery. Lake boundaries were visually digitized using Panchromatic Band-8, at a nominal spatial resolution of 15 m, based on the relative contrast between the dark, water-filled lakes and the surrounding ice, which has relatively higher reflectance. A clear and consistent set of guidelines were employed in order to ensure consistency and quality in selecting lake features for manually mapping lakes from Landsat ETM+ imagery. First, only lake features large enough to reasonably discern lake boundaries were captured. Smaller lake features close to either the nominal spatial resolution or less than the average width of missing rows were not captured. Lakes that were either completely or significantly eclipsed by missing scan lines were not mapped resulting in a minimum lake size of $\sim$7000 m^2 captured by this method. Additionally, rectilinear features, indicative of a stream or stream like structures were not mapped. Lake mapping was executed through protocols that involved two independent analysts for quality control. A total of 1180 (filled) lakes were mapped from three Landsat-7 scenes acquired on 6 June, 22 June, and 9 August 2007 (Lampkin, forthcoming).

Surface velocity data

Surface velocity estimates were derived from the RADARSAT satellite platform. SAR interferometric pairs were used to estimate velocities for 2000, 2004, 2005, and 2006 over the Jakobshavn outlet basin (Farness and Jezek, 2008). Velocity grids for the 2006 season were

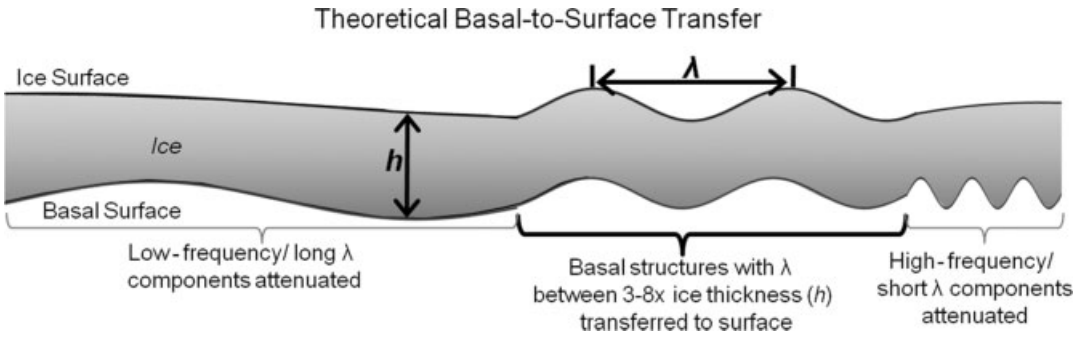

Figure 2. Schematic of basal to surface transfer as a function of ice thickness, where (h) is ice thickness and (λ) indicates surface and basal wavelength (not drawn to scale). Basal wavelength (λ) components between three and eight times the ice thickness (h) are most readily transferred through the ice whereas wavelengths longer and shorter than this 3–8× window are strongly attenuated

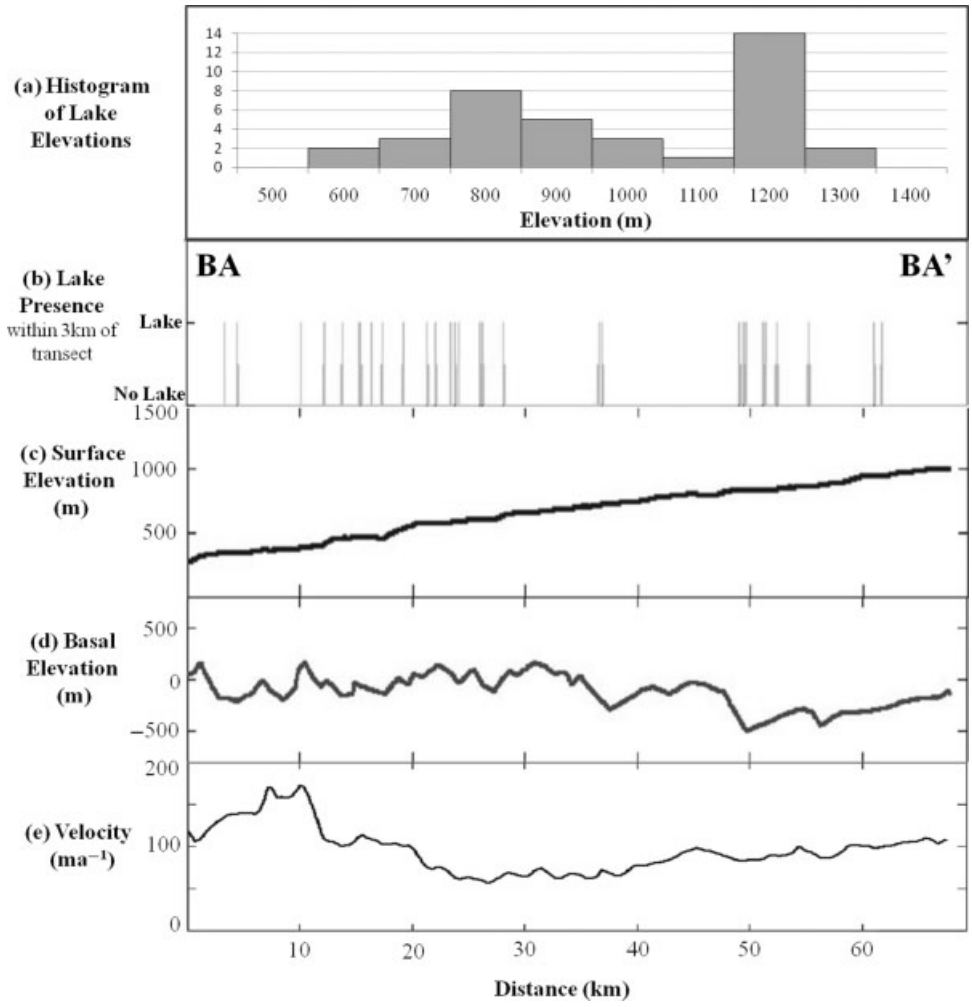

Figure 3. a) Histogram showing elevation distribution of analysed lakes: b) Longitudinal profile of lake locations mapped laterally onto the transect from BA to BA' and analysed using the spatial autocorrelation to determine periodicity of the lake distribution. c) Surface topographic profile along the transect. 3d) Basal topographic profile along the transect. This figure shows the spatial distribution of lakes as they relate to basal and surface topography

used for this analysis and acquired from the CReSIS data archive (https://www.cresis.ku.edu/data/satellite-measurements). Velocity grids for the 2007 season were not available due to poor coherence between interferometric pairs, resulting in poor velocity retrievals.

The transect of focus in this study was selected based on three criteria: orientation, proximity to lakes, and proximity to the Jakobshavn ice stream. The transect was selected based on its orientation being parallel to ice flow, to avoid the influence of spatial anisotropy in the surface topography (Gudmundsson, 2003; Smith *et al.*, 2006). This transect was also located near numerous lakes, ensuring an adequate sample size for analysis. And finally, this transect was located far from the margins of the Jakobshavn ice stream channel to avoid impact of strong velocity gradients, which can complicate the

transfer of basal roughness to the surface topographic structure. Additionally, the margins of the ice stream tend to be devoid of supraglacial lakes.

METHODS

This study uses several methods to characterize the frequency structure in basal and surface topography and their relationship to supraglacial lake distribution along a 65 km long transect located south of the Jakobshavn ice stream (Table I). Fourier transform was applied to both surface and basal elevation profiles to calculate the power spectra. Fourier transform removes all spatial information; therefore wavelet decomposition was also applied to delineate the spatial distribution of the power spectra. An autocorrelation analysis was used to evaluate periodicity in the occurrence of supraglacial lakes near the study transect. Lastly, an assessment of the relative impact of basal sliding to that of internal deformation, along the transect, on basal-to-surface roughness transfer will be explored. An estimate of depth-averaged velocity due to internal deformation will be calculated and compared to measured surface velocity derived from SAR to determine where basal sliding dominates ice flow.

Fourier and wavelet decomposition, and basal and surface topography

Basal and surface profiles were examined using spectral analysis through the application of Fourier decomposition. The Fourier transform and characteristic spectra for the basal topographic profile were compared to surface spectra along the transect in order to quantify frequencies that propagate through the ice and those that have been filtered. In this analysis, the Discrete Fourier Transform (DFT) was applied to surface and basal profiles, given by

$$X(k) = \sum_{j=1}^{N} x(j) e^{-2\pi i(j-1)(k-1)/N},\ j = 1, 2, \ldots N \qquad (2)$$

where detrended, profiles $x(j)$ of N elements were input for $i = \sqrt{-1}$. The Fourier decomposition can be informative, because it provides high resolution information about the distribution of spectral components within the surface and basal signals. Unfortunately, there is a loss of localized spatial information. Given this limitation, wavelet decomposition was applied to surface and basal elevation data to derive a wavelet power spectrum. Wavelet analysis indentifies the distribution of power across a range of frequencies (wavelengths) at discrete intervals along the length of the profile. A continuous wavelet transform (cwt) was applied to discrete sequence (x_η), or detrended basal and surface elevation profiles, where x_η is convolved with a scaling function (s) and translated (η) Morlet wavelet function (ψ) (Daubechies, 1990, 1992; Trauth, 2010), given by:

$$W_\eta(s) = \sum_{\eta'=0}^{N-1} X_{\eta'\psi} \times \left[\frac{(\eta' - \eta)\delta d}{s}\right] \qquad (3)$$

for equal spatial increments δd along the profiles, where ψ (* indicate the complex conjugate),

$$\psi_o(\eta) = \pi^{-1/4} e^{i\omega o\eta} e^{-\eta 2/2} \qquad (4)$$

describing a Morlet wavelet that is a plane wave modulated by a Gaussian of non-dimensional frequency (ω_o). Scaling parameters were set ($75 < s < 4400$) to high values based on the number of points present in the dataset, resulting in highly stretched wavelets, resolving low-frequency components which tend to dominate the frequency spectra of both surface and basal profiles.

Comparison of basal and surface wavelet power spectra will indicate the distribution of frequencies transferred into the ice sheet surface structure as a function of ice thickness along the profile of interest.

This study quantifies the spatial periodicity of supraglacial lakes within the vicinity of the basal/surface topographic profile through estimating the autocorrelation or correlogram of lake features along the length of the transect, where the autocorrelation coefficient (r_w) is estimated at discrete lags w (Box *et al*., 1994), given by

$$r_w = c_w / c_o \qquad (5)$$

where c_w is the autocovariance and c_o variance functions,

$$C_w = (1/N) \sum_{t=1}^{N-k} (X_t - \mu)(X_{(t+w)} - \mu),\ w = 1, 2, \ldots K \qquad (6)$$

and

$$c_o = (1/N) \sum_{t=1}^{N} (X_t - \mu)^2 \qquad (7)$$

for X_t and the next sample X_{t+w} for a total of K samples along the profile, where μ is the mean basal and surface elevations along the transect. A radius of 3 km was used to buffer the profile from which lakes were sampled from the supraglacial lake inventory constructed during the 2007 melt season. A 3 km radius was selected because it was sufficiently large to provide a reasonable sample of lakes, and assumed to be at a distance where the basal topography along the transect would still influence the transverse surface topography. A sample of 38 lake features were extracted from within the 3 km buffer

Table I. Summary of spectra analysis of the relationships among supraglacial lake distribution, surface topography, and basal topography by various methods along the BA to BA' transect

Data	Method	Dominant frequencies	
Supraglacial akes	Autocorrelation	11 km	5·6 km
Surface topography	Fourier	10 km	
	Wavelet	10–11 km	~5 km
Basal topography	Fourier	10 km	~5 km
	Wavelet	10–11 km	~5 km

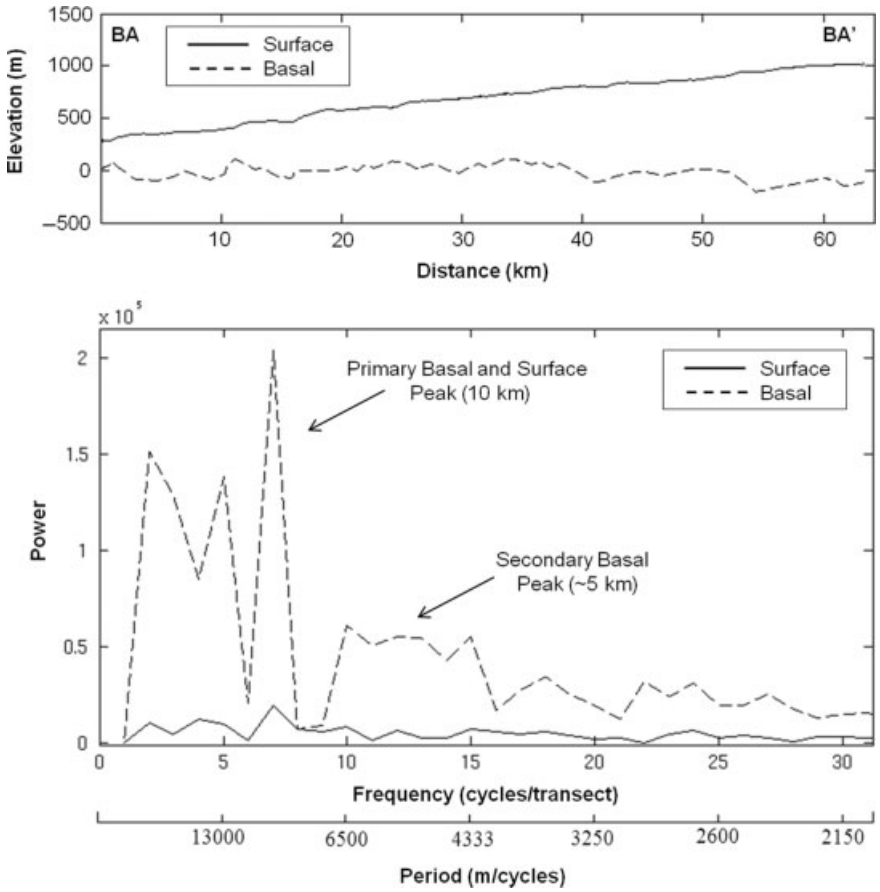

Figure 4. (Top) Basal and surface topography profiles; (bottom) Fourier analysis of basal and surface topographies, where (y) axis is spectra power and (x) axis is frequency (cycles/transect) or Period (meters/cycle). Both basal and surface profiles exhibit dominant signals at frequencies corresponding to features of 10 km in length. Basal topography shows a broad secondary peak ranging between 4·5 and 6·5 km

(Figures 1c and 3b). This sample represents a subset of lakes derived from the entire Landsat lake archive, which included 1180 mapped lakes. The 38 lakes represent filled lakes mapped from Landsat scenes acquired on 6 June, 22 June, and 9 August 2007. The location of each of the 38 lake features were horizontally mapped onto the basal/surface transect. The mapping of lake locations to the transect in this manner allows for direct comparison of lake locations to roughness components in the basal and surface topography as well as ice thickness along the study transect.

Estimation of depth-averaged velocity

The total velocity at the surface of a glacier is due to internal deformation and basal sliding, expressed as

$$u = u_d + u_b \tag{8}$$

Surface velocity can be prescribed from retrieved SAR data, such that $u = u_{SAR}$, and the deformation component is commonly derived assuming laminar flow conditions, where the shear strain rate and shear stress are related through Glen's Flow Law (Glen, 1955), given by

$$\dot{\varepsilon}_{\mathrm{XZ}} = \mathrm{A}\tau^{n}{}_{xz} \tag{9}$$

where A is the temperature-dependent flow law parameter, n is an empirically determined constant, and τ_{xz} is the shear stress at depth, expressed as

$$\tau_{\mathrm{xz}} = \rho g(h - z)\sin\theta \tag{10}$$

ρ is the density of ice, g is acceleration due to gravity and θ is the surface gradient in the x-direction (Patterson, 1994). Integrating with respect to z, for $n = 3$, depth-average velocity ($\overline{u}_d$) is given by (Van der Veen, 1999)

$$\overline{u}_d = \frac{2}{n+2}(\rho \mathrm{g}\theta)^3 h \tag{11}$$

where $u_d = \overline{u}_d$. Estimates of $\overline{u}_d$ are derived assuming ice deforms by horizontal shearing along planes parallel to the ice surface, and that all other forces in the force balance but shear stress are zero. These assumptions indicate that horizontal gradients in surface and bedrock topography are much smaller than vertical gradients (Hutter, 1983). CReSIS-derived ice thickness, and surface slopes derived from the SPOT DEM were input to Equation (11). The difference (U^*) between u_{SAR} and $\overline{u}_d$ was calculated to quantify the relative influence of basal sliding along the transect.

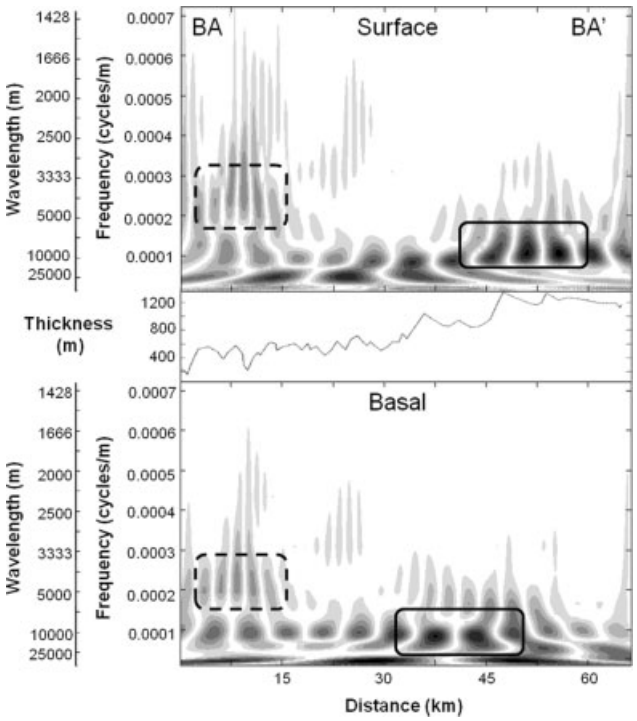

Figure 5. Wavelet analysis of basal (bottom) and surface (top) topography along transect plotted with ice thickness (middle) from BA (left) to BA' (right). Grey-scale represents strength of in power at specific locations. Both basal and surface wavelets exhibit significant power at 10–11 km (black solid line box) wavelengths over thicker ice and ~5 km (black dashed line box) over thinner ice. Shift in high power regions in both the surface and basal spectra may be related to upstream surface compression relative to a downstream region where the basal topography is rough and ice velocities are slower

RESULTS

Spectral analysis of basal and surface topography

Fourier power spectra (Figure 4) demonstrates two dominant frequencies in the basal topography corresponding to undulations at $\lambda \approx 10$ km and $\lambda \approx 4{\cdot}5 < \lambda < 6{\cdot}5$ km. The basal topography also contains some strength at very low frequencies. Fourier decomposition of the surface topography identifies an identical peak at $\lambda = 10$ km. Additionally, basal topography tends to have greater power in higher frequency components than surface topography.

Wavelet analysis (Figure 5) of the basal topography also identifies a strong peak between $10 < \lambda < 11$ km, as well as a broad secondary peak around 5 km. Wavelet decomposition of the surface identifies the same peaks in power between 10 and 11 km, and again, a broad secondary peak around 5 km λ. Also important is the distribution of power across varying wavelengths (frequencies) along the transect. Wavelengths within the 10–11-km range tend to dominate surface structure over thicker ice, whereas undulations near 5 km are more dominant over thinner ice. Both the Fourier and the Wavelet analyses consistently indicate wavelength components in both the basal and surface topographies around 5 and 10–11 km.

Spatial autocorrelation of lakes

Spatial autocorrelation of the supraglacial lake distribution produces five peaks of correlation of; 1·9, 5·6, 11, 24, and 31 km (Figure 6), of which 5·6 and 11 km correspond with frequencies identified in the basal and surface profiles. This indicates that lake distribution is not random and that it is responsive to several frequency components present in the basal topography.

Influence of basal sliding

Application of Equations (8) and (11) to the study transect indicate relatively stronger control on ice speeds due to internal deformation over basal sliding between ~30–45 km upstream (Figure 7). The highest values in U^*, measured in percent difference, indicate substantial departure from internal deformation dominated flow along the lower limb of the transect (along the first 20 km) and at limited sections along the highest elevations of the transect (~ between 50 and 60 km). These regions along the transect have flow that is dominated by basal sliding and correspond to locations where lakes are present. The region along the transect where internal deformation is dominant, corresponds to a region that has fewer lakes that are also less clustered (>45 km and <30 km) (Figure 3b). This result seems to suggest that the presence of lakes is correlated with regions dominated by basal sliding over internal deformation.

DISCUSSION AND CONCLUSIONS

Results suggest lake distribution is responsive to two dominant basal frequencies dependent upon ice thickness. Over thicker ice (1200–1400 m) the 10–11 km frequency component dominates and influences lake distribution. The 10–11 km frequency component is very near 8 times longer than the 1200–1400 m ice thickness which shows that lakes distribution is responsive to frequencies at the high end of Gudmundsson's (2003) transfer window of 3–8 times ice thickness (1250 m $\times$ 8 = 10 km/1400 m $\times$ 8 = 11 km). Over thinner ice (500–700 m), lake distribution exhibits the strongest

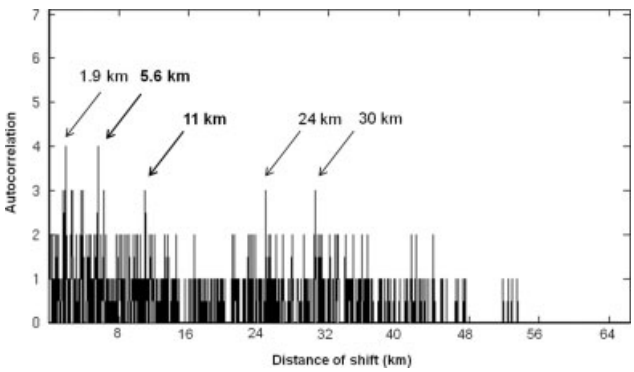

Figure 6. Spatial autocorrelation of supraglacial lakes. Peaks indicate highest level of spatial periodicity along the transect. Strongest peaks are noted with corresponding wavelengths. Wavelengths of 5·6 and 11 km (bold arrows) are also found in the Fourier and Wavelet analysis of basal topography

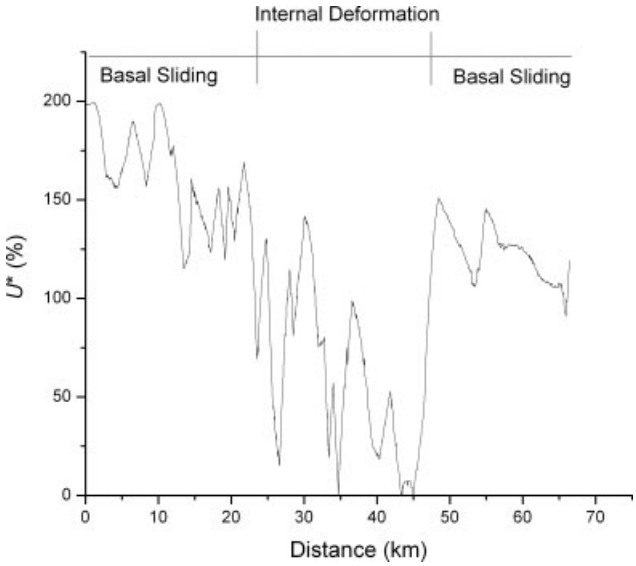

Figure 7. Relative impact of basal sliding (u_b) to internal deformation (u_d) on ice sheet velocity along the study transect through calculation of U^* (percent difference) between measured surface velocity (u) and an estimate of u_d based on the depth-average velocity. High values in U^* indicate the relative importance of basal sliding to surface velocity over internal deformation

periodicity of 5·6 km, which is very near 8 times the ice thickness (625 m × 8 = 5 km). These results experimentally support Gudmundsson's (2003) window of transfer as a function of ice thickness. Generally, it has been established that basal topography tends to have greater power in higher frequency components than surface topography. The lack of these higher-frequency basal components at the surface has been attributed to attenuation due to internal deformation (Whillans and Johnsen, 1983). Results indicate that basal sliding dominates the lower elevation section of the study transect, corresponding to surface undulations with the highest power near the 5·6 km frequency. There are surface undulations at lower elevations with significant power near the 1·9 km frequency that is less prevalent in the basal topography and may not be directly attributed to basal influence.

Frequencies in lake distributions that are either less than or greater than theoretical limits established by Gudmundsson (2003) may indicate other processes. Lake distribution generally correlates with depressions in bedrock topography, with some variation which may be explained by exogenic processes. The transfer of basal undulation to the surface is regulated by not only ice thickness but drag variation at the bed in addition to the vertical distribution of ice viscosity Gudmundsson (2003). Surface undulations at wavelengths that are less than the ice thickness can be influenced by surface–atmosphere processes such as accumulation, ablation, and redistribution (Smith, 2005). The transect analysed in this study does not contain wavelengths in the surface structure that are less than the ice thickness, even though there are relatively higher frequencies present in the surface profile between 0 and 15 km that have less power in the basal profile (present in the wavelet power spectrum). There is relatively stronger power in the lower elevation section of the surface transect ($\lambda \approx 2$ km) than the basal transect, where ice thickness varies between 400 and 500 m. The presence of high-frequency components in this part of the transect might be indicative of amplified short wavelength transfer due to enhanced basal sliding. This has been theoretically proposed, where the slip ratio demonstrates reduced drag at the bed (more sliding) than the impact of internal deformation (Gudmundsson, 2003). Basal-to-surface frequency transfers modulated by bedrock/ice interface conditions would surely manifest in a phase shift between basal and surface roughness elements, but to adequately interpret these shifts, it would be necessary to know if the ice is frozen to the bed, what the distribution of till is, and if the till is saturated or frozen. We currently do not have such data along the particular transect used in this analysis.

This work presents preliminary results and future efforts are required to expand this analysis to other regions within the greater Jakobshavn drainage basin. Additional work will explore enhanced basal-to-surface transfer under increased basal sliding due to surface drainage; as such a process may represent an important feedback mechanism that has currently been overlooked. Forthcoming ice penetrating radar retrievals of the bed/ice sheet state (frozen *vs* decoupled) will provide additional insight into the basal-to-surface roughness transfers. There is also a need to identify regions within the ablation zone, where surface roughness components are more strongly modulated by surface-atmosphere processes, relative to sub-surface transfer processes. This, and future work, will further constrain the influence of basal topography of surface roughness and its corresponding impact on supraglacial lake distribution.

ACKNOWLEDGMENTS

This study is supported by NASA (Grant Number NNX10AG18G). We would like to acknowledge Drs Sridhar Anandakrishnan and Richard Alley of the Department of Geoscience, Pennsylvania State University, for their constructive input, and the Pennsylvania State Ice and Climate group (PSICE). We would also like to acknowledge the technical support and feedback Joel Plummer provided on the Center for Remote Sensing of Ice Sheets (CReSIS) basal topography dataset.

NOTATIONS

The following symbols are used in this paper:

$X(k)$ = Fourier transform*
$W_\eta(s)$ = Continuous wavelet transform*
ε_{xz} = Strain rate along x-direction*
$\overline{z}$ = Vertical depth (m)*

REFERENCES

Alley RB, Clark PU, Huybrechts P, Joughin I. 2005a. Ice-sheet and sea-level changes. *Science* **310**(5747): 456.

Alley RB, Dupont TK, Parizek BR, Anandakrishnan S. 2005b. Access of surface meltwater to beds of sub-freezing glaciers: preliminary insights. *Annals of Glaciology* **40**: 8–14.

Bartholomew I, Nienow P, Mair D, Hubbard A, King MA, Sole A. 2010. Seasonal evolution of subglacial drainage and acceleration in a Greenland outlet glacier. *Nature Geoscience*.

Boon S, Sharp M. 2003. The role of hydrologically-driven ice fracture in drainage system evolution on an Arctic glacier. *Geophysical Research Letters* **30**(18): 1916.

Box GE, Jenkins GM. 1994. *Time Series Analysis: Forecasting and Control*. 3rd edn, Upper Saddle River: Prentice-Hall, NJ.

Box JE, Ski K. 2007. Remote sounding of Greenland supraglacial melt lakes: implications for subglacial hydraulics. *Journal of Glaciology* **53**(181): 257–265.

Budd WF. 1968. The longitudinal velocity profile of large ice masses. *IASH Publications* **79**: 58–77.

Budd WF. 1969. The dynamics of ice masses. ANARE Scientific Reports. Ser. A(IV). Glaciology. No. 108.

Budd WF. 1970. Ice flow over bedrock perturbations. *Journal of Glaciology* **9**(55): 29–48.

Budd WF, Carter DB. 1971. An analysis of the relation between the surface and bedrock profiles of ice caps. *Journal of Glaciology* **10**(9): 197–209.

Das SB, Joughin I, Behn MD, Howat IM, King MA, Lizarralde D, Bhatia MP. 2008. Fracture Propagation to the Base of the Greenland Ice Sheet During Supraglacial Lake Drainage. *Science* **320**(5877): 778–781.

Daubechies I. 1990. The wavelet transform time-frequency localization and signal analysis. *IEEE Transactions on Information Theory* **36**: 961–1004.

Daubechies I. 1992. *Ten Lectures on Wavelets.* Society for Industrial and Applied Mathematics, Philadelphia, p. 357.

Dowdeswell JA. 2006. The Greenland ice sheet and global sea-level rise. *Science* **311**: 963–964.

Echelmeyer K, Clarke TS, Harrison WD. 1991. Surficial glaciology of Jakobshavn Isbrae, West Greenland. I: Surface morphology. *Journal of Glaciology* **37**(127): 368–382.

Farness K, Kenneth J. 2008. *Velocity Trends for Jakobshavn Glacier, Greenland for the Years 2000, 2004, 2005, and 2006 including Procedure Manuals.* BPRC Technical Report No. 2008-01, Byrd Polar Research Center, The Ohio State University: Columbus, Ohio; p. 60.

Fountain AG. 2005. Fractures as the main pathways of water flow in temperate glaciers. *Nature* **433**(7026): 618.

Glen JW. 1955. The creep of polycrystalline ice, *Proceedings of the Royal Society of London, Series A* **228**: 519–538.

Gudmundsson GH. 2003. Transmission of basal variability to a glacier surface. *Journal of Geophysical Research-Solid Earth* **108**(B5): 2253.

Hardy RJ, Bamber JL, Orford S. 2000. The delineation of drainage basins on the Greenland ice sheet for mass-balance analyses using a combined modelling and geographical information system approach. *Hydrological Processes* **14**(11): 1931–1941.

Howat IM, Smith BE, Joughin I, Scambos TA. 2008. Rates of southeast Greenland ice volume loss from combined ICESat and ASTER observations, *Geophysical Research Letters* **35**(17): L17505.

Hutter K. 1983. *Theoretical glaciology: material science of ice and the mechanics of glaciers and ice sheets.* D. Reidel Publishing Co: Dordrecht.

Hutter K, Legerer F, Spring U. 1981. First order stresses and deformations in glaciers and ice sheets, *Journal of Glaciology* **27**: 227–270.

Intergovernmental Panel on Climate Change. 2007. *Climate Change 2007: The Physcial Science Basis*. *Contribution of Working Group I to the Fourth Assessment Report of the Intergovernmental Panel on Climate Change*, Solomon S, Qin D, Manning M, Chen Z, Marquis M, Averyt KB, Tignor M, Miller HL. New York: Cambridge Univ. Press: Cambridge, UK. Kenneally.

Jezek KC, Drinkwater M, Crawford J, Bindschadler R, Kwok R. 1993. Analysis of synthetic aperture radar data collected over the southwestern Greenland ice sheet. *Journal of Glaciology* **39**(131): 119–132.

Joughin I, Das SB, King MA, Smith BE, Howat IM, Moon T. 2008. Seasonal speedup along the western flank of the Greenland Ice Sheet. *Science* **320**(5877): 781.

Joughin I, Smith BE, Howat IM, Scambos T, Moon T. 2010. Greenland flow variability from ice-sheet-wide velocity mapping. *Journal of Glaciology* **56**(197): 415–430.

Joughin I, Abdalati W, Fahnestock M. 2004. Large fluctuations in speed on Greenland's Jakobshavn Isbrae glacier. *Nature* **432**(7017): 608–610.

Luckman A, Murray T. 2005. Seasonal variation in velocity before retreat of Jakobshavn Isbrae, Greenland. *Geophysical Research Letters* **32**(8).

Luckman A, Murray T, De Lange R, Hanna E. 2006. Rapid and synchronous ice-dynamic changes in East Greenland. *Geophysical Research Letters* **33**(3).

Luthje M, Pedersen LT, Reeh N, Greuell W. 2006. Modelling the evolution of supraglacial lakes on the West Greenland ice-sheet margin. *Journal of Glaciology* **52**(179): 608–618.

McMillan M, Nienow P, Shepherd A, Benham T, Sole A. 2007. Seasonal evolution of supra-glacial lakes on the Greenland ice sheet. *Earth and Planetary Science Letters* **262**(3): 484–492.

Nye JF. 1959. A method of determining the strain-rate tensor at the surface of a glacier. *Journal of Glaciology* **3**(25): 409–418.

Paterson WSB. 1994. *Physics of Glaciers* (3rd edn). Pergamon Press: New York.

Parizek BR, Alley RB. 2004. Implications of increased Greenland surface melt under global-warming scenarios: ice-sheet simulations. *Quaternary Science Reviews* **23**(910): 1013–1027.

Plummer J, Gogineni S, van der Veen C, Leuschen C, Li J. 2008. Ice Thickness and bed map 462 for Jakobshavn Isbrae, *CReSIS Tech Report* #2008-1.

Rignot E, Kanagaratnam P. 2006. Changes in the velocity structure of the Greenland Ice Sheet. *Science* **311**(5763): 986.

Shepherd A, Hubbard A, Nienow P, King M, McMillan M, Joughin I. 2009. Greenland ice sheet motion coupled with daily melting in late summer. *Geophysical Research Letters* **36**(1): L01501.

Smith BE, Raymond CF, Scambos T. 2006. Anisotropic texture of ice sheet surfaces. *Journal of Geophysical Research* **111**(F1): F01019.

Smith BE. 2005. Characterization of the small scale topography of Antarctica and Greenland, (Ph.D. Thesis, Univ. of Washington).

Stearns LA, Hamilton GS. 2007. Rapid volume loss from two East Greenland outlet glaciers quantified using repeat stereo satellite imagery. *Geophysical Research Letters* **34**(5): 5503.

Sundal AV, Shepherd A, Nienow P, Hanna E, Palmer S, Huybrechts P. 2009. Evolution of supra-glacial lakes across the Greenland Ice Sheet. *Remote Sensing of Environment* **113**(10): 2164–2171.

Thomas R, Frederick E, Krabill W, Manizade S, Martin C. 2009. Recent changes on Greenland outlet glaciers. *Journal of Glaciology* **55**(189): 147–162.

Thomsen HH, Thorning L, Braithwaite RJ. 1988. *Glacier-hydrological conditions on the inland ice north-east of Jakobshavn/Ilulissat, west Greenland*, Gronlands Geologiske Undersogelse.

Trauth M H. 2010. *MATLAB recipes for Earth Sciences*, 3rd ed., Springer-Verlag Berlin Heidelberg.

Van den Broeke M, Bamber J, Ettema J, Rignot E, Schrama E, Van de Berg WJ, Van Meijgaard E, Velicogna I, Wouters B. 2009. Partitioning recent Greenland mass loss. *Science* **326**(5955): 984.

Van der Veen CJ. 1998. Fracture mechanics approach to penetration of surface crevasses on glaciers. *Cold Regions Science and Technology* **27**(1): 31.

Van der Veen CJ. 1999. In *Fundamentals of Glacier Dynamics*, Lisse AA (ed), Balkema: Rotterdam/Brookfield; p. 462.

Van der Veen CJ. 2007. Fracture propagation as means of rapidly transferring surface meltwater to the base of glaciers. *Geophysical Research Letters* **34**(1): L01501.

Velicogna I. 2009. Increasing rates of ice mass loss from the Greenland and Antarctic ice sheets revealed by GRACE, *Geophysical Research Letters* **36**(19): L19503.

Weertman J. 1973. Can a water-filled crevasse reach the bottom surface of a glacier. *IASH Publications* **95**: 139–145.

Whillans IM, Johnsen SJ. 1983. Longitudinal variations in glacial flow: theory and test using data from the Byrd Station strain network, Antarctica. *Journal of Glaciology* **29**(101): 78–97.

Zwally HJ, Abdalati W, Herring T, Larson K, Saba J, Steffen K. 2002. Surface melt-induced acceleration of Greenland ice-sheet flow. *Science* **297**(5579): 218.

